# Central Lancashire Online Knowledge (CLoK)

Title	Design and analysis of a novel dual source vapor injection heat pump using exhaust and ambient air
Type	Article
URL	https://clok.uclan.ac.uk/id/eprint/38798/
DOI	https://doi.org/10.1016/j.enbenv.2020.11.004
Date	2020
Citation	Li, Jing, Fan, Yi, Zhao, Xudong, Bai, Xiaoman, Zhou, Jinzhi, Badiei, Ali, Myers, Steve and Ma, Xiaoli (2020) Design and analysis of a novel dual source vapor injection heat pump using exhaust and ambient air. Energy and Built Environment. ISSN 2666-1233
Creators	Li, Jing, Fan, Yi, Zhao, Xudong, Bai, Xiaoman, Zhou, Jinzhi, Badiei, Ali, Myers, Steve and Ma, Xiaoli

It is advisable to refer to the publisher's version if you intend to cite from the work.
https://doi.org/10.1016/j.enbenv.2020.11.004

For information about Research at UCLan please go to http://www.uclan.ac.uk/research/
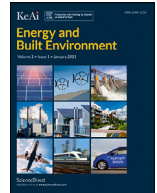
Design and analysis of a novel dual source vapor injection heat pump using exhaust and ambient air

Jing Li [a], Yi Fan [a], Xudong Zhao [a,*], Xiaoman Bai [b], Jinzhi Zhou [c], Ali Badiei [a], Steve Myers [a], Xiaoli Ma [a]

[a] Research Centre for Sustainable Energy Technologies, University of Hull, Hull HU6 7RX, UK
[b] Environment Design Centre, School of Art and Medium, Hefei Normal University, Hefei 230601, China
[c] School of Mechanical Engineering, Southwest Jiaotong University, Chengdu, Sichuan, PR China

ARTICLE INFO

ABSTRACT

A novel dual source vapor injection heat pump (DSVIHP) using exhaust and ambient air is proposed. The air exhausted from the building first releases energy to the medium-pressure evaporator and is then mixed with the ambient air to heat the low-pressure evaporator. A vapor injection (VI) compressor of two inlets is connected with the low and medium pressure evaporators. It's first time that a VI compressor is employed to recover the ventilation heat. The system can minimize the ventilation heat loss and provide a unique defrosting approach by using the exhaust waste heat. Fundamentals of the proposed DSVIHP are illustrated. Mathematical models are built. Both energetic and exergetic analyses are carried out under variable conditions. The results indicate that the DSVIHP has superior thermodynamic performance. The superiority is more appreciable at a lower ambient temperature. It has a higher COP than the conventional vapor injection heat pump and air source heat pump by 11.3% and 23.2% respectively at an ambient temperature of -10 °C and condensation temperature of 45 °C. The waste heat recovery ratio from the exhaust air is more than 100%. The novel DSVIHP has great potential in the cold climate area application.

1. Introduction

Demand for a reduction of fossil fuel consumption and carbon emission in relation to building heating is urgent and mandatory. New target has been set in the UK to bring all greenhouse gas emissions to net zero by 2050, updated from the previous target of at least 80% reduction from 1990 levels [1]. At present, approximately 85% of UK households and 65% of non-domestic buildings depend on gas boiler systems [2]. Low carbon heating systems including heat pump, biomass, solar and combined micro heat and power units are still subordinate, reaching only 2% of the overall heating market. A fundamental shift away from the use of natural gas is required to meet the new target.

Heat pump systems represent an increasing market share in the building heating and cooling segment owing to attractive payback period [3], good integrability into facades [4], high efficiency [5], large renewable energy contribution when combined with solar panels [6,7] and potential in various applications [8]. A market share of 100% of the systems could be achieved for new houses in many countries where the heat pump technology is well-established and domestic hot water supply by solar is mandatory [9]. About 90% of heat pump systems use air as heat source in the UK [10]. One serious problem of an air source heat

pump (ASHP) for space heating in winter is the frosting on the outdoor coil surface, which leads to increased fan power [11], deteriorate heat transfer [12] and reduced heating capacity [13]. The efficiency is low since a large amount of electricity is consumed for periodic defrosting.

Aside from employment of ASHP, waste heat recovery is an efficient approach to energy saving in buildings. A substantial proportion of the building energy loss is through ventilation, typically more than 30% for a social home [14]. The ratio is even higher for public and commercial buildings such as hospitals, schools, restaurants and supermarkets. In active heat recovery, exhaust air heat pumps (EAHP) are commonly used to extract heat from discharge air, with the heat being pumped into the fresh supply air, or supplied to a heating element within the interior of the building [15]. A number of studies on the control strategy[16], combination with solar and ground energy [17,18], effect on district energy use [19], annual performance [20] and thermo-economic performance [21] have been carried out. Compared with other types of exhaust heat recovery methods such as thermal wheel, an EAHP eliminates cross contamination between fresh and exhaust air, and is able to achieve a high recovery efficiency of more than 100% without reheating the fresh air [22]. The EAHPs have been commercialized. Nevertheless, a challenge of EAHP is the limited heating capacity, resulting in a high capital cost

ARTICLE IN PRESS

JID: ENBENV [m5GeSdc;December 2, 2020;9:19]

J. Li, Y. Fan, X. Zhao et al. Energy and Built Environment xxx (xxxx) xxx

per kW and long payback time. About 15000 brand new social homes were equipped with EAHPs in the UK between 2009 and 2013, most owners and housing association tenants had reported increased electricity bills [23]. The recovery of the waste heat of exhaust air is inadequate to meet the entire building energy demand because there are heat losses through windows, walls and roofs in addition to ventilation heat loss. Auxiliary heating devices e.g. electric or gas heater are required to provide domestic hot water, compensate for other heat losses and cover peak loads [16].

In order to make use of exhaust air from the building and reduce the dependence on auxiliary heating devices, a novel dual source vapor injection heat pump (DSVIHP) is proposed in this paper. It takes advantages of large heating capacity of conventional ASHP and high efficiency of EAHP. The exhaust air is first used to heat a medium-pressure evaporator and with a reduced temperature it is further mixed with the ambient air for the heating of a low-pressure evaporator. The low and medium pressure evaporators are connected to the two inlets of a vapor injection (VI) compressor. This novel DSVIHP has the potential to produce heat efficiently for domestic hot water supply and space heating with a large capacity.

Heat pumps using both exhaust and ambient air as the heat source have been reported in the literature [24,25], in which a conventional compressor of one inlet and one outlet is adopted and the two types of air are mixed directly. The mixture has a higher temperature than the ambient and therefore the frost time can be prolonged in winter operation. However, the direct mixing process results in a significant thermodynamic irreversibility as there is generally a temperature difference of about 20 °C between the exhaust and ambient air. A more thermodynamically efficient combination of the two types of air has yet to be proposed.

To the best of the authors' knowledge, it is first time that a VI compressor is employed for the waste heat recovery of exhaust air in this paper. Cascade utilization of the exhaust air is devised via two-stage evaporators, leading to a reduced irreversibility in the mixing process. Simulation is implemented on the DSVIHP. Comparison with conventional air source heat pumps is made. The influences of ambient temperature, condensation temperature, vapor inject temperature and mass flow ratio of ambient and exhaust air on the heat pump performance are investigated.

2. System description

The proposed DS-VIHP is illustrated in Fig. 1. It comprises a vapor injection compressor, condenser, internal heat exchanger (IHX), medium-pressure (MP) evaporator, low-pressure (LP) evaporator, MP and LP throttle valves.

2.1. Fundamentals

The refrigerant leaving the condenser is split into two streams. One is throttled via the MP valve with a decreased temperature and the other directly flows into the IHX. The refrigerant from the MP valve is at binary phase state. It first absorbs heat from the exhausted air with an elevated quality, and then is completely vaporized in the IHX. The other stream is subcooled and then throttled via the LP valve. The refrigerant is vaporized by the mixture of exhaust and outdoor air in the LP evaporator. The two streams flow to the medium and low pressure inlet ports of the vapor injection compressor, respectively. The vapor is compressed and then condensed in the condenser. The refrigerant circulates. The waste heat is first recovered through the MP evaporator and the exhaust air at a reduced temperature is further mixed with the ambient air. In addition, the DSVIHP system comprises a mixing chamber for receiving and mixing the exhaust and ambient air. The mixture is used to heat the LP evaporator.

The pressure-enthalpy (*p-h*) diagram of the heat pump is presented in Fig. 2. Compared with a conventional vapor injection heat pump

(VIHP), the novel heat pump has an additional evaporator (MP evaporator), where the refrigerant is partially vaporized by the exhaust air, as denoted by the process from State point 2 to 3. The vapor injection rate is therefore increased, offering a higher COP.

A possible design of the DSVIHP is displayed in Fig. 3. The mass flow rates in the LP and MP evaporators may be controlled in correspondence with the ambient air temperature, exhaust air temperature, condensation temperature, power of the compressor and consumers' demand on space heating and domestic hot water. The MP and LP throttle valves may be controlled to regulate the mass flow rates in the first and second streams, respectively.

2.2. Advantages

Compared with a conventional air source heat pump, vapor injection heat pump and exhaust air heat pump, the novel DSVIHP has some foreseeable advantages, including:

First, the use of a second evaporator (MP evaporator) enables additional heat to be recovered from the exhaust air, beyond what would be recovered with only a single stage evaporator heat recovery process. In a conventional EAHP, the exhaust air leaving the evaporator may have a relatively high temperature for the sake of an acceptable COP, leading to an insufficient waste heat recovery. While in the proposed heat pump, the utilization of exhaust air is improved by the two-stage evaporators. The air is discharged from the heat pump at a lower temperature than the ambient.

Second, the system has flexible operation modes. The mass flow rates of exhaust air and ambient air are adjustable. By using exhaust air, the problem of frosting is substantially reduced compared with a conventional air source heat pump, because the exhaust air leaving the MP evaporator is warmer than ambient and the heat source temperature for the LP evaporator is elevated. Further, even if the LP evaporator becomes frosted with ice, that ice may be removed by stopping the flow of ambient air into the mixing chamber, so that the ice is melted by the heat in the exhaust air flow. In regard to a temperature difference of about 20°C between the exhaust air and ice, an efficient defrosting process is anticipated. The ventilation can be enhanced if faster defrosting is needed. Accordingly, the use of exhaust air flow mixed with the ambient air flow can reduce the energy consumption of the heat pump system compared with a conventional ASHP, in conditions susceptible to frosting.

Third, it is more suited to producing domestic hot water than a standard heat pump, for which the minimum temperature requirement is about 60 °C to kill legionella bacteria. It can successfully tackle the challenges especially during the night-time operation. The ambient temperature in winter nights in the UK can fall below -5 °C, which is too low for a standard ASHP to supply heat efficiently and a large amount of electricity is also consumed for defrosting. The novel DSVIHP is much more appropriate in this situation due to the two-stage compression. The consumer's bill will be significantly reduced by using off-peak electricity.

3. Mathematical model

In the simulation, R410A (a zeotropic but near-azeotropic mixture of R32 and R125, 50%/50%) is adopted. The coefficient of performance (*COP*) of the heat pump is the ratio of heat gain to electricity consumption,

$$COP = \frac{Q_{hp}}{W_e} \tag{1}$$

Q_{hp} and W_e are the heat supply and power input, kW.

The ventilation heat loss without recovery is

$$Q_{ven} = m_{ex}C_P\left(T_{ex} - T_{am}\right) \tag{2}$$

where m_{ex}, C_P, T_{am} and T_{ex} are exhaust air flow rate (kg/s), heat capacity (J/kg/°C), ambient temperature and temperature of exhaust air leaving
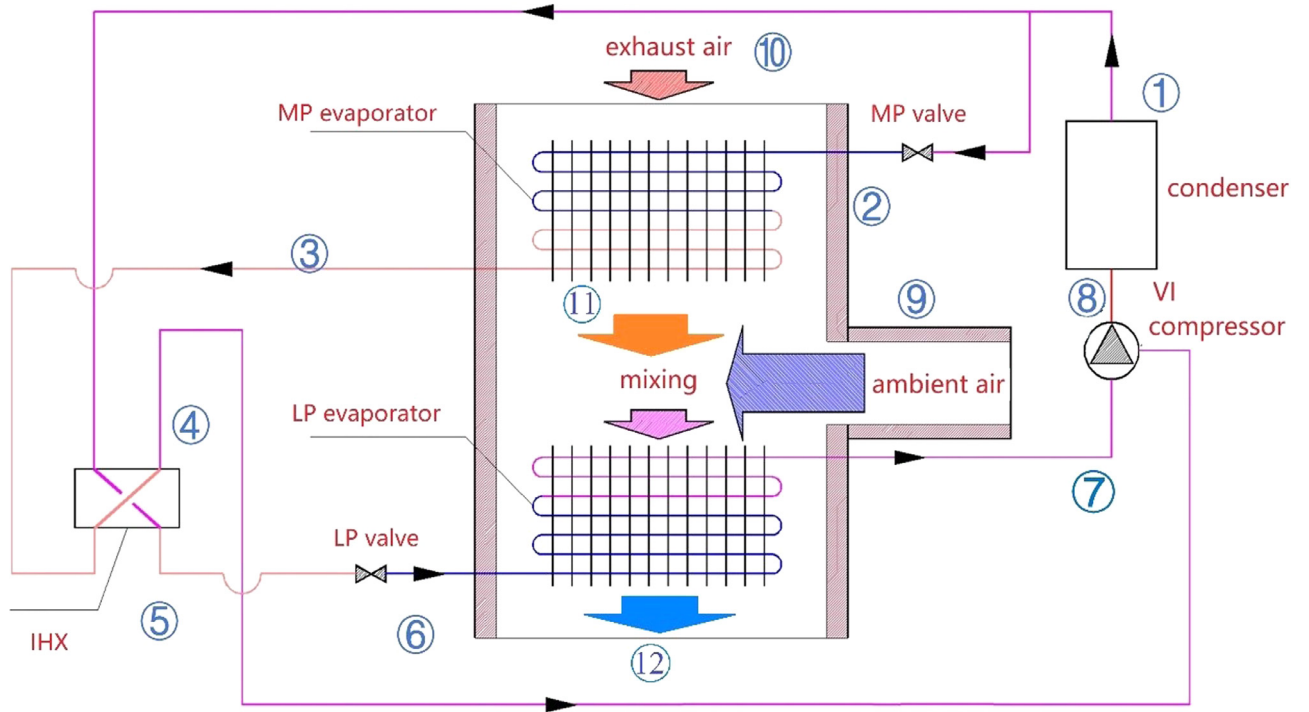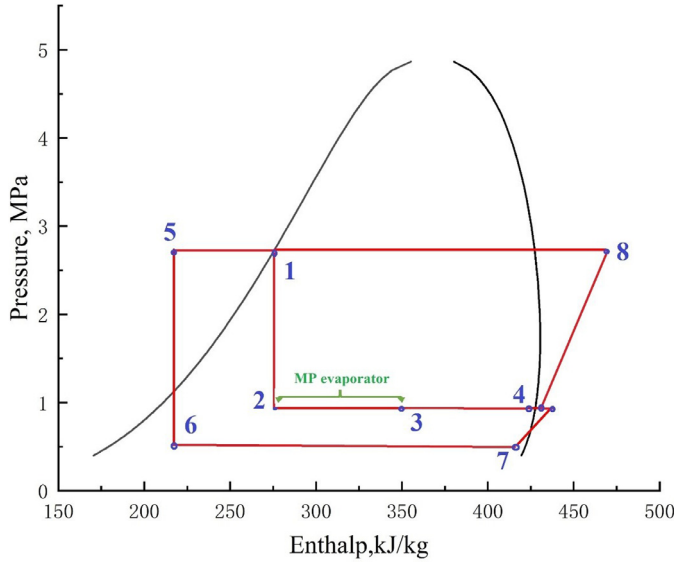
ARTICLE IN PRESS

JID: ENBENV [m5GeSdc;December 2, 2020;9:19]

J. Li, Y. Fan, X. Zhao et al. Energy and Built Environment xxx (xxxx) xxx

Fig. 1. Schematic diagram of the DSVIHP.

Fig. 2. *p-h* diagram of the DSVIHP.

Table 1

Exergy destruction equations for the main components of the DS-VIHP.

Component	Equation
Condenser	$[\mathbf{m}_{R410A,1}(\mathbf{s}_1 - \mathbf{s}_8) + \mathbf{m}_w(\mathbf{s}_{w,out} - \mathbf{s}_{w,in})]\mathbf{T}_0$
MP throttle valve	$\mathbf{m}_{R410A,3}(\mathbf{s}_2 - \mathbf{s}_1)\mathbf{T}_0$
LP throttle valve	$\mathbf{m}_{R410A,6}(\mathbf{s}_6 - \mathbf{s}_5)\mathbf{T}_0$
MP evaporator	$[\mathbf{m}_{R410A,3}(\mathbf{s}_3 - \mathbf{s}_2) + \mathbf{m}_{ex}(\mathbf{s}_{11} - \mathbf{s}_{10})]\mathbf{T}_0$
LP evaporator	$[\mathbf{m}_{R410A,6}(\mathbf{s}_7 - \mathbf{s}_6) + (\mathbf{m}_{ex} + \mathbf{m}_{am})\mathbf{s}_{12} - \mathbf{m}_{am}\mathbf{s}_9 - \mathbf{m}_{ex}\mathbf{s}_{11}]\mathbf{T}_0$
Internal heat exchanger	$[\mathbf{m}_{R410A,3}(\mathbf{s}_4 - \mathbf{s}_3) + \mathbf{m}_{R410A,6}(\mathbf{s}_5 - \mathbf{s}_1)]\mathbf{T}_0$
Compressor	$(\mathbf{m}_{R410A,1}\mathbf{s}_8 - \mathbf{m}_{R410A,6}\mathbf{s}_7 - \mathbf{m}_{R410A,3}\mathbf{s}_4)\mathbf{T}_0$

are the mass flow rate of exhaust air and ambient air. The flow rates of the two streams in the refrigerant cycle are $m_{R410A,3}$ and $m_{R410A,6}$ ($m_{R410A,3} + m_{R410A,6} = m_{R410A,1}$).

4. Results and discussion

In this simulation, the influences of the ambient temperature, condensation temperature, vapor injection temperature, mass flow ratio of ambient air to exhaust air and type of refrigerant on the performance of the DSVIHP are analysed. Comparison with a conventional VIHP and ASHP is implemented. Some assumptions are made: (1) compressor efficiency of 0.8, (2) minimum temperature difference of 5 °C for heat transfer in the LP and MP evaporators, condenser and internal heat exchanger, (3) air temperature drop of 5 °C for the LP evaporator of the DSVIHP, and evaporators of VIHP and ASHP, (4) exhaust air flow rate of 1.0 kg/s, (5) refrigerant of R410A for Sections 4.1–4.4, 4.6 and R134a for Section 4.5. The fan power is not included and the pressure drop of refrigerant in the heat exchangers are neglected. For the assumed exhaust air flow rate of 1.0 kg/s, the value might be larger than that of a common residential house. Notably, the proposed system is also applicable in public buildings, such as hospital, library, office and school where the heating demand is large. A flow rate of 1.0 kg/s can be reasonable.

the building (°C), respectively. The ratio of the ventilation heat loss to the heat supply is defined as

$$x = \frac{Q_{ven}}{Q_{hp}} \tag{3}$$

Because there is a mixing process, the mass flow ratio of ambient air to exhaust air is expressed by

$$y = \frac{m_{am}}{m_{ex}} \tag{4}$$

An insight to the thermodynamic irreversibility in the innovative DSVIHP is provided. The exergy destruction in the components is expressed in Table 1. The subscripts '1–12' represent the thermodynamic states in Fig. 1. T_0 is the reference temperature, 0 °C. m_{ex} and m_{am}
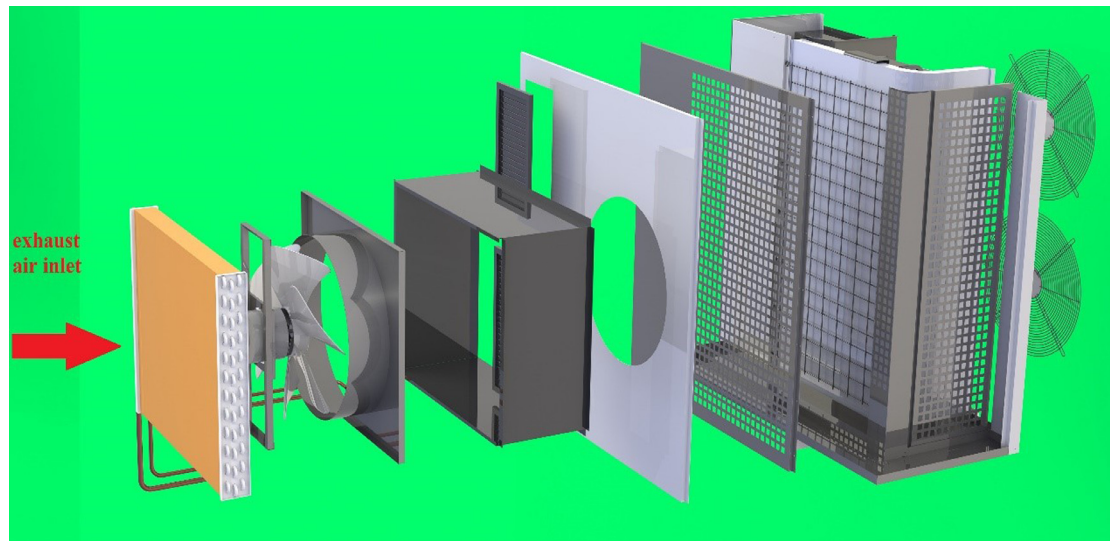
(a)

Mixture leaving heat pump

Ambient air inlet

MP evaporator

(b)

Fig. 3. Design diagram of the proposed DSVIHP: (a) components; (b) external view.

4.1. Influences of ambient temperature

A comparison among the COPs for the innovative DSVIHP, convectional VIHP and ASHP is presented in Fig. 4 at variable ambient temperature. The condensation temperature for all the heat pumps is 45 °C. For the DSVIHP, the air flow rate of ambient air, vapor injection temperature (T_2) are 6 kg/s and 5 °C. The COP of the DSVIHP ranges from about 3.72 to 4.16 when the ambient temperature increases from -10 to 0 °C, and it is 3.34 to 3.88 for the VIHP and 3.02 to 3.61 for the ASHP. It is obvious that the innovative heat pump has a higher COP and the advantage is more remarkable at a lower ambient temperature. For example, the relative COP increment over that of the VIHP and ASHP is 11.3% and 23.3% respectively at -10 °C. Two reasons can be given for the higher COP: First, the DSVIHP has a larger vapor injection ratio than the convectional VIHP. The mass flow ratio of the injected to the uninjected refrigerant ($m_{R410A,3}/m_{R410A,6}$) at -5 °C is 79.23% for the DSVIHP, which

is about twice that of the VIHP (39.89%). The DSVIHP can be deemed as a combination of a VIHP using ambient air as the heat source and an ASHP using exhaust air as the heat source. It has a higher equivalent temperature in the vaporization process than the VIHP due to the heat input from the exhaust air. Second, the exhaust air leaving the MP evaporator still has a higher temperature than the ambient air. The mixture elevates the evaporation temperature in the LP evaporator. A detailed parameter distribution of the DSVIHP at an ambient temperature of -5 °C is provided in Table 2. Given a temperature of mixture leaving the LP evaporator of -7.8 °C, the waste heat recovery from the exhaust air is about 111%. The waste heat recovery ratio is higher than that of a conventional exhaust air heat pump.

The power input of the compressor and temperature drop of ambient air through the LP evaporator varying with the ambient temperature for the DSVIHP are depicted in Fig. 5. Given the mass flow rates of the exhaust and ambient air, the evaporation pressure in the LP evapora-

ARTICLE IN PRESS

JID: ENBENV   [m5GeSdc;December 2, 2020;9:19]

J. Li, Y. Fan, X. Zhao et al.   Energy and Built Environment xxx (xxxx) xxx

Table 2
Parameter distribution of the DSVIHP at an ambient temperature of -5 °C.

State point	Fluid	Flow rate ,kg/s	Temperature, °C	Pressure, MPa	Enthalpy, kJ/kg	Quality, %
1	R410A	0.308	45.0	2.733	275.85	0
2	R410A	0.136	5.03	0.936	275.85	31.68
3	R410A	0.136	5.07	0.936	348.83	65.59
4	R410A	0.136	5.10	0.936	422.84	100
5	R410A	0.172	11.23	2.733	217.21	subcooled
6	R410A	0.172	-12.83	0.520	217.21	15.39
7	R410A	0.172	-12.75	0.520	417.02	100
8	R410A	0.308	74.69	2.733	468.75	superheated
9	outdoor air	6.0	-5.0	0.1	394.26	superheated
10	exhaust air	1.0	20.0	0.1	419.41	superheated
11	exhaust air	1.0	10.1	0.1	409.45	superheated
12	mixed air	7.0	-7.8	0.1	391.45	superheated
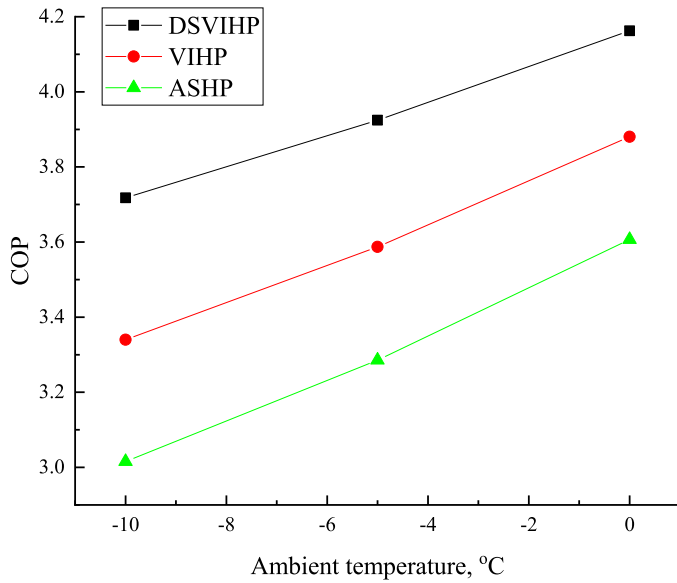
Fig. 4. COP variations with the ambient temperature for the DSVIHP, conventional VIHP and ASHP.
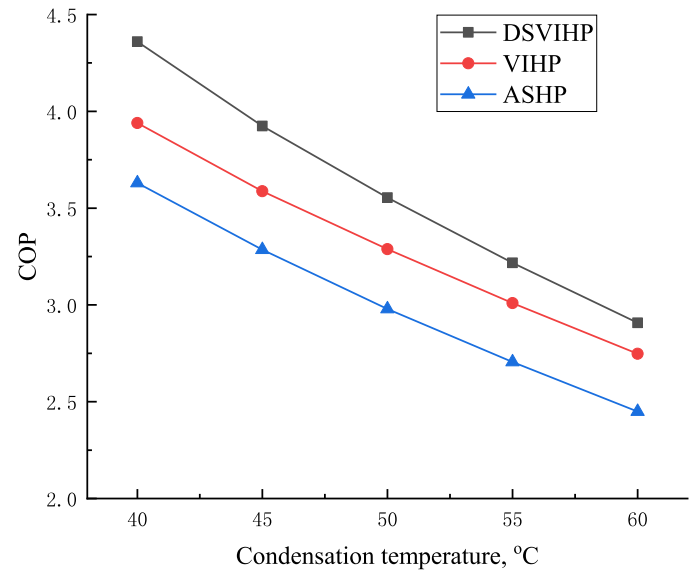
Fig. 6. Variations of the COPs of the DSVIHP, conventional VIHP and ASHP with the condensation temperature.
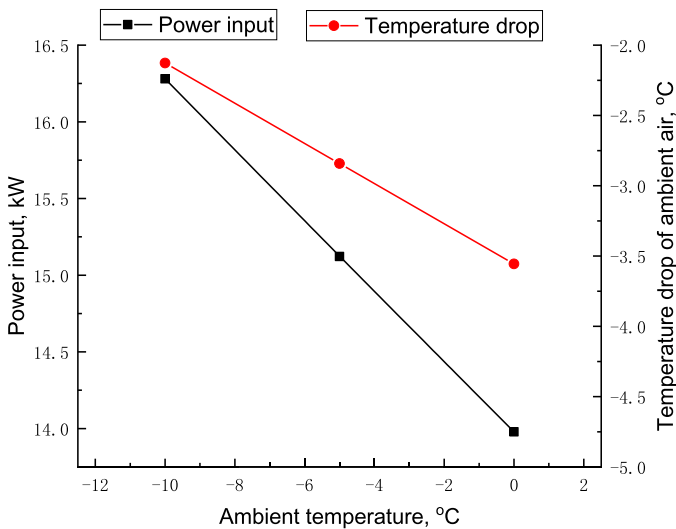
Fig. 5. Variations of the power input and temperature drop with the ambient temperature for the DSVIHP, conventional VIHP and ASHP.

tor rises with the increment in the ambient temperature, leading to a lower power input. Although the temperature drop of 5 °C of the mixture through the LP is independent on the ambient temperature, the temperature drop of the ambient air from the entrance to the exit is actually less than 5 °C (2–3 °C as shown in the figure). This can be explained by an increased temperature of the ambient air after a mixing process with the exhaust air.

4.2. Influences of condensation temperature

COP variations for the three types of heat pumps with the condensation temperature are displayed in Fig. 6. The ambient temperature is -5 °C. The air flow rate of ambient air and vapor injection temperature for the DSVIHP are the same as those in Section 4.1. The COP decreases with the increment in the condensation temperature. However, the decrements are different, which are 1.45, 1.19, 1.18 for the DSVIHP, VIHP and ASHP respectively when the condensation temperature increases from 40 to 60 °C. The relative decrements are 33.3%, 30.2% and 32.5%. At a higher condensation temperature, the novel heat pump still has a higher efficiency but the superiority becomes less appreciable. The results indicate that the DSVIHP is more preferable in applications of relatively low condensation temperature and ambient temperature. For example, in northern China where the ambient temperature in winter can be lower than -10 °C, the DSVIHP will be desirable for an underfloor heating unit of inlet temperature of about 40 °C.
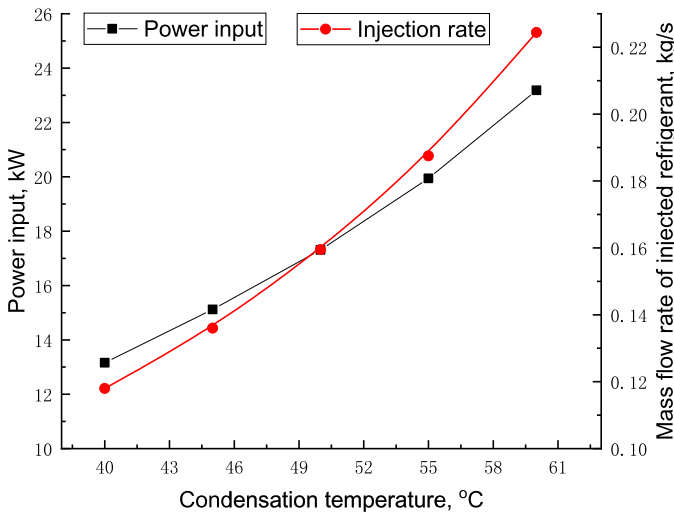
Fig. 7. Variations of the power input and mass flow rate of injected R410A with the condensation temperature for the DSVIHP.
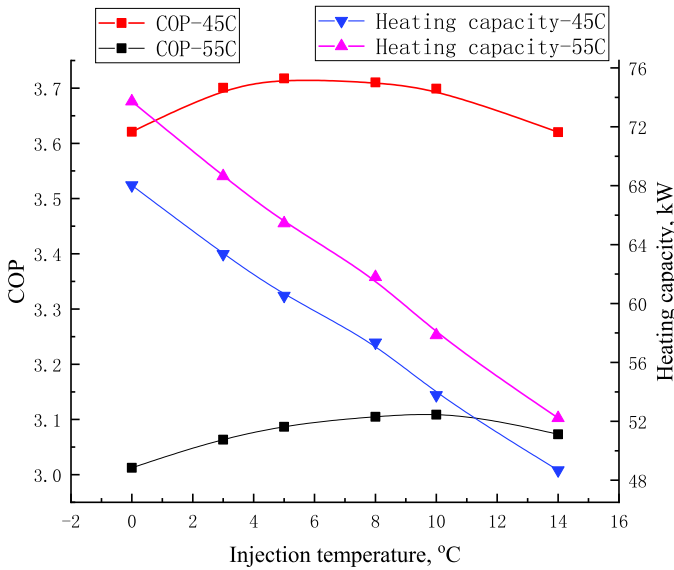

Fig. 8. Variations of COP and heat supply with the injection temperature for the DSVIHP.

The DSVIHP has a higher COP than a conventional VIHP due to the utilization of exhaust air. In contrast to the ambient temperature, the condensation temperature does not have impact on the waste heat utilization. As the condensation temperature rises, temperatures of the exhaust air leaving the MP evaporator and the mixture leaving the LP evaporator are not changed. The increasing condensation temperature will only lead to increments in the compressor power consumption and mass flow rate of injected refrigerant ($m_{R410A,3}$), as shown in Fig. 7, which is similar with the situation in a conventional VIHP. As a result, the COPs of the DSVIHP and VIHP get closer at a higher condensation temperature.

4.3. Influences of vapor injection temperature

Aside from the ambient temperature and condensation temperature, the vapor injection temperature (T_2) affects the performance of the DSVIHP, as shown in Fig. 8. The ambient temperature is -10 °C and the condensation temperature is 45 °C and 55 °C, respectively. The injection temperature varies from 0 to 14 °C. A maximum COP appears at T_2 of
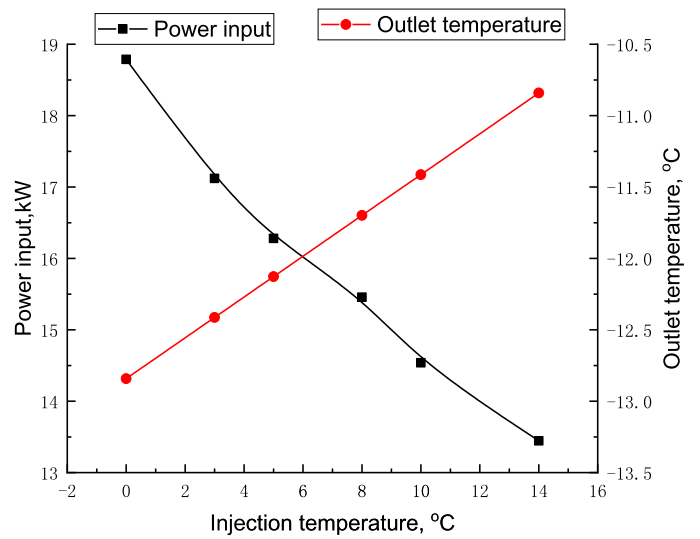

Fig. 9. Variations of the power input and outlet temperature of mixture leaving the LP evaporator with the injection temperature for the DSVIHP.

about 5 °C when the condensation temperature is 45 °C. A higher injection temperature can increase the mixture temperature of the exhaust and ambient air and reduce the difference between evaporation and condensation temperature, which has a positive impact on the COP. However, the waste heat recovery from the exhaust air in the MP evaporator and vapor injection ratio are decreased. For instance, $m_{R410A,3}/m_{R410A,6}$ can drop from 114.37% to 34.13% with the increment in T_2. Due to the compromise between the evaporation temperature and injection ratio, there is an optimum injection temperature. The optimum temperature goes up as the condensation temperature increases. It is about 10 °C at a condensation temperature of 55 °C.

Unlike the COP, the heating capacity decreases monotonically as the injection temperature increases. It ranges from 63.6 to 48.6 kW and 73.7 to 52.2 kW for the condensation temperature of 45 and 55 °C respectively. Given mass flow rates of exhaust and ambient air of 1.0 and 6.0 kg/s, a higher T_2 is accompanied with a lower heat input through the MP evaporator. The temperature of air mixture is elevated, resulting in a higher evaporation temperature in the LP evaporator. The mass flow rate of the injected R410A and input power of the compressor are decreased as shown in Fig. 9 for a condensation temperature of 45 °C. The results indicate that a higher injection temperature is more suitable at a larger proportion of the ventilation heat loss to the total building energy losses. It is also deduced that if the exhaust air from buildings is mixed directly with the ambient air to heat the LP evaporator for which the injection temperature is close to 20 °C, the heat supply of the heat pump will be small with a low COP.

4.4. Influences of mass flow ratio of ambient air to exhaust air

Variations of the COP and heat supply of the DSVIHP with the mass flow ratio of the ambient air and exhaust air (y) are shown in Fig. 10. The ambient temperature, condensation temperature and vapor injection temperature are -10, 45 and 5 °C. Given the mass flow of the exhaust air (1.0 kg/s) and the temperature drop (5 °C) of the mixture through the LP evaporator, a higher y leads to more heat input to the LP evaporator. The mass flow rate of R410A in the LP evaporator and the heating capacity are thereby increased. Because the exhaust air leaving the MP evaporator is almost constant (10 °C), an increment in y also results in a decrement in the mixture temperature. The outlet temperature of the mixture declines from about -11 to -13 °C when y increases from 5 to 10, as shown in Fig. 11.
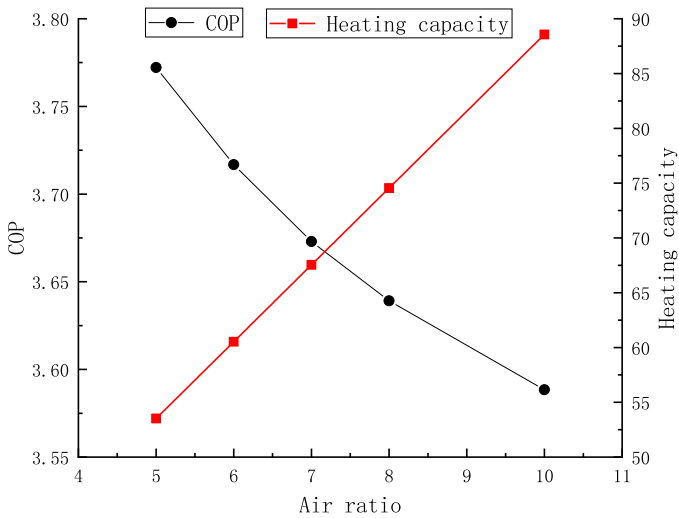
Fig. 10. Variations of the COP and heat supply with the air flow ratio for the DSVIHP.
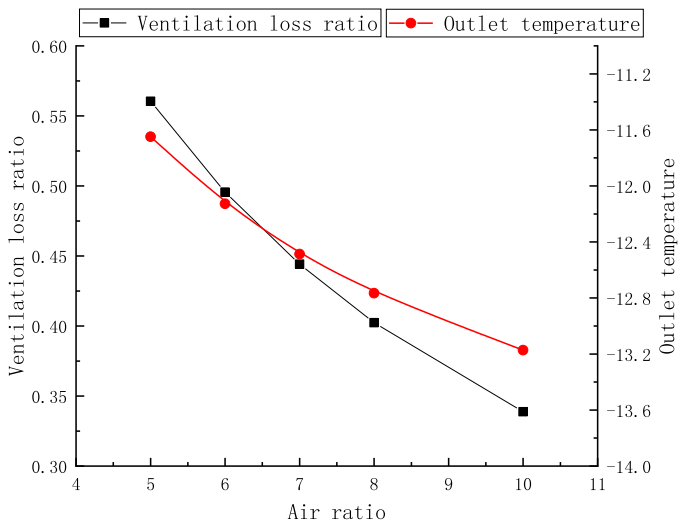

Fig. 11. Variations of the ventilation heat loss ratio (x) and outlet temperature of the mixture with the air flow ratio for the DSVIHP.

With a larger R410A flow rate in the LP evaporator, the COP falls down since the average evaporation temperature of the DSVIHP decreases. The ratio of the ventilation heat loss to the heat supply (x) also drops from about 56% to 33%.

4.5. 4.5 Influences of refrigerant

Similar with other heat pump systems, the DSVIHP system has refrigerant as a key component. The refrigerant has an important impact on the thermodynamic performance. The parameters of the cycle using R134a (1,1,1,2-Tetrafluoroethane) are provided in Table 3. The condensation temperature, ambient temperature, vapor injection temperature, mass flow rates of exhaust air and ambient air are same as those in Table 2, but the pressure, enthalpy, quality of the refrigerant are different. R134a is expected to be widely used in the heat pump industry for next decade due to its favorable thermodynamic and thermo-physical properties [26,27]. It has a higher COP than R410A (4.1 Vs 3.9). However, R134a has a lower saturation pressure and larger specific volume at a given temperature. Its saturation vapor volume is 0.107 m^3/kg at -12 °C, while it is only 0.049 m^3/kg for R410A. The volume that needs to be swept by the compressor is significantly larger and therefore higher
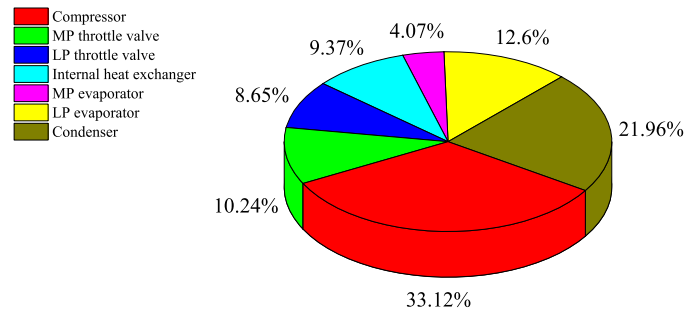

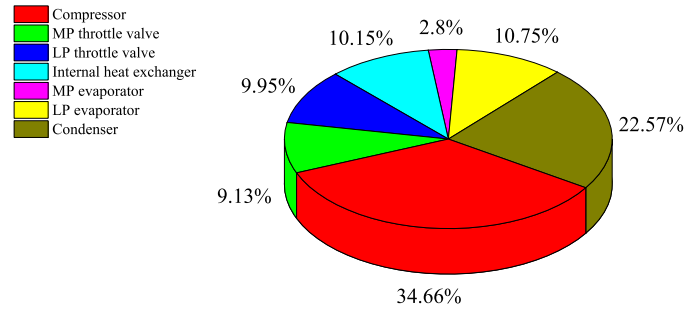Fig. 12. Exergy destruction in the DSVIHP at $y = 6$.

Fig. 13. Exergy destruction in the DSVIHP at $y = 10$.

investments are needed for installation. The selection of the refrigerant is a compromise among the thermodynamic performance, environmental impact and cost.

4.6. Thermodynamic irreversibility in the components

The thermodynamic irreversibility in the components is revealed in Fig. 12. The ambient temperature, condensation temperature, vapor injection temperature and air flow ratio are -10 °C, 45 °C, 5 °C and 6, respectively. The largest exergy destruction takes place in the compressor, which amounts for about one third of the total system losses. It is followed by the destruction in the condenser owing to a large heat transfer irreversibility between the superheated refrigerant and cooling water.

The total exergy loss in the throttle valves (LP and MP valves) is less than that in the compressor and the ratio of the former to the latter is about 58%. As a comparison, for a conventional ASHP operating at a condensation temperature of 45 °C and ambient temperature of -10 °C, the ratio of the exergy destruction in the throttle valve to that in the compressor is about 142%, indicating the thermodynamic irreversibility during throttling is much more remarkable. The novel DSVIHP is able to reduce the exergy destruction in the valves by two means: (1) The refrigerant leaving the condenser is split into two streams. The irreversibility of the first stream in the MP throttle valve is weakened due to a higher pressure at the outlet of the valve. (2) The second stream is supercooled prior to the expansion. The irreversibility in the LP throttle valve is reduced by a lower quality and specific volume of the refrigerant. The quality of R410A at the LP valve outlet is only 17%, while is about 43% for that in a conventional ASHP under a similar condition. The throttling is an adiabatic process, and the exergy destruction can be determined by $\int_{p1}^{p2} vdp$. A lower pressure drop and specific volume will diminish the losses. The exergy losses in the components vary with the air flow ratio. As shown in Fig. 13, when y increases to 10, there are slight increments in the compressor and condenser losses and decrements in the valve losses.

Table 3
Parameter distribution of the DSVIHP using R134a.

State point	Fluid	Flow rate, kg/s	Temperature, °C	Pressure, MPa	Enthalpy, kJ/kg	Quality, %
1	R134a	0.342	45.0	1.160	263.94	0
2	R134a	0.143	5.0	0.350	263.94	29.37
3	R134a	0.143	5.0	0.350	333.87	65.28
4	R134a	0.143	5.0	0.350	401.49	100
5	R134a	0.199	11.29	1.160	215.46	subcooled
6	R134a	0.199	-12.86	0.179	215.46	15.64
7	R134a	0.199	-12.86	0.179	390.93	100
8	R134a	0.342	58.69	1.160	437.12	superheated
9	outdoor air	6.0	-5.0	0.1	394.26	superheated
10	exhaust air	1.0	20.0	0.1	419.41	superheated
11	exhaust air	1.0	10.0	0.1	409.45	superheated
12	mixed air	7.0	-7.8	0.1	391.45	superheated

Fig. 14. Prototype of the novel DSVIHP.

5. Future work

A prototype of the DSVIHP has been developed, as shown in Fig. 14. It has a heating capacity of about 5 to 10 kW. The refrigerant is R410A. It flows around a streamed circuit, recovering heat from exhaust air flowing through the heat pump system. Installation on the Applied Science Building in University of Hull has been completed. Experimental tests will be conducted in the coming winter and more work will be reported in the near future.

Aside from the experimental validation, future works will be conducted on the thermo-economic performance. The proposed DSVIHP uses exhaust air for defrosting without additional electricity consumption. Its seasonal performance factor is anticipated to be higher than that of a conventional ASHP, leading to a lower operational cost. It can recover the ventilation heat and meet the building thermal energy demand. It is a combination of ventilation heat recovery system and heat pump. For conventional ventilation recovery technologies, thermal wheel, plate heat exchanger, run-around-coil and heat pipe generally have an efficiency of about 70%, 60%, 47% and 57%, respectively [28]. On the assumptions of an average exhaust air flow rate of 0.2kg/s, a proportion of ventilation loss to total building heat loss (x) of 33% and an ambient temperature of -10 °C, the total heat demand of the house will be about 18 kW. If a plate heat exchanger of an efficiency of 60% and an ASHP of a COP of 3.0 (shown in Fig. 4) are employed, the heat

supply and electricity consumption by the ASHP will be about 14.4 and 4.8 kW, respectively. Given a COP of 3.59 as depicted in Fig. 10, the electricity will be 5.0 kW if the proposed DSVIHP is used. The electricity saving is comparable to the side-by-side heat recovery system and ASHP in the normal condition. Since a conventional ASHP is likely to suffer from frosting in winter and consume significant electricity for defrosting, the annual electricity saving of the DSVIHP shall be higher than that of the side-by-side systems.

The development of the DSVIHP is supported by a UK project to reduce the carbon emission. It has the potential to replace gas boilers for space heating. The DSVIHP may be also applicable in areas where space cooling is needed in summer. In the cooling mode as depicted in Fig. 15, all the components (compressor, condenser, evaporators, internal heat exchangers and throttle valves) working in the heating mode are still in operation. There are some changes in the flow direction. The condenser in Fig. 1 is turned into the evaporator and the chilled water flows to the underfloor cooling unit in the building. The MP evaporator in Fig. 1 becomes a subcooler. The refrigerant leaving the compressor is first condensed by the air mixture and then cooled down by the exhaust cold air from the building. The subcooled refrigerant is split into two streams: one is throttled via the MP valve and then completely vaporized by the IHX (green line); the other is further cooled down by the IHX, throttled via the LP valve and vaporized (blue line). The subcooler can increase the cooling capacity of refrigerant per kg in the evaporator and the mix-
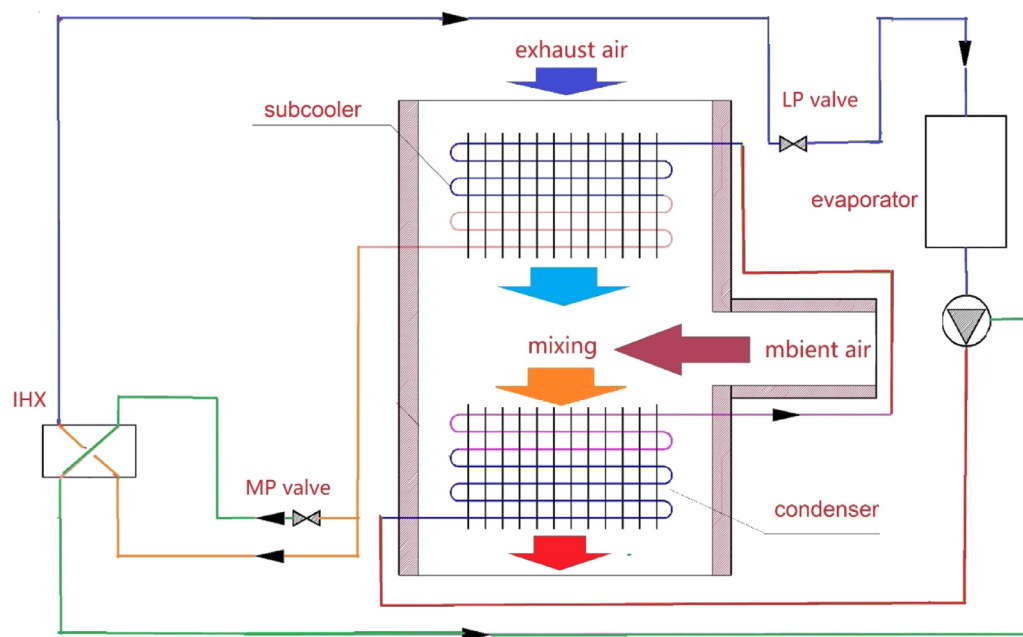
ARTICLE IN PRESS

JID: ENBENV [m5GeSdc;December 2, 2020;9:19]

J. Li, Y. Fan, X. Zhao et al. Energy and Built Environment xxx (xxxx) xxx

Fig. 15. Flow chart of the system in the cooling mode.

ture can decrease the condensation temperature. Through the two-stage utilization of the exhaust air, the energy efficiency ratio (EER) of the DSVIHP will be higher than a conventional ASHP in summer.

6. Conclusion

More heat pump systems are expected to replace coal and gas boilers in China, UK and other countries in an attempt to tackle the escalating climate crisis. Compared to existing heat pump technologies, this proposed system comprises unique features. It is first time that vapor injection heat pump has been used to recover waste heat of exhaust air from the buildings. The new system overcomes two technical challenges:

1 Minimizing the ventilation heat loss. Unlike a conventional EAHP that extracts energy from exhaust air to heat the fresh supply air, the DSVIHP uses both exhaust and outdoor air as the heat sources. It has a higher heating capacity at a given mass flow rate of exhaust air and the waste heat recovery ratio is more than 100%. By recovering the ventilation heat loss, the DSVIHP can saved about 23% of electricity consumption as compared with a conventional ASHP at normal operation conditions of condensation temperature of 45 °C and ambient temperature of -10°C.

2 Defrosting of heat pump in cold climate areas. The DSVIHP has flexible operation modes. In the defrosting mode for which the vents for the ambient air are shut down, the DSVIHP provides a promising solution to frosting by using the exhaust waste heat without additional electricity consumption. The seasonal performance factor is expected to be significantly higher than that of a conventional ASHP regarding to the near-zero electricity consumption for defrosting.

3 The performance of the DSVIHP is affected by the ambient temperature, condensation temperature, vapor injection temperature and air flow ratio. A lower ambient temperature will increase its advantages over conventional air source heat pump and vapor injection heat pump. Increment in the condensation temperature leads to decrement in the COP but has no impact on the waste heat recovery. The optimum vapor injection temperature is about 5 °C at an ambient temperature of - 10°C, which increases as the condensation temperature rises. The flow ratio of the ambient air to the exhaust air influences the COP and heating capacity. A higher flow ratio is accompanied with a lower proportion of ventilation heat loss.

4 The largest exergy destruction takes place in the compressor, which accounts for about a third of the total exergy losses in the DSVIHP. This is followed by the exergy destruction in the condenser (about 20%) and LP evaporator (about 10%). Among the components, the MP evaporator has the least exergy destruction. In all the simulation scenarios, the proposed heat pump is most beneficial under the conditions of an ambient temperature of about -10°C and condensation temperature of about 40-45°C

Credit author statement

Jing Li: Conceptualization, Methodology, Simulation, Writing. Yi Fan: Visualization, Drawing. Xudong Zhao: Supervision, Writing-Reviewing and Editing. Xiaoman Bai: Drawing, Literature Survey. Jinzhi Zhou: Discussion, Writing-Reviewing and Editing. Ali Badiei: Discussion. Steve Myers: Discussion. Xiaoli Ma: Discussion.

Declaration of Competing Interest

The authors declare that they have no known competing financial interests or personal relationships that could have appeared to influence the work reported in this paper.

Acknowledgment

Reference

[1] UK becomes first major economy to pass net zero emissions law. https://www.gov.uk/government/news/uk-becomes-first-major-economy-to-pass-net-zero-emissions-law, 20200510.

[2] BEIS - Clean Growth: Transforming Heating. https://assets.publishing.service.gov.uk/government/uploads/system/uploads/attachment_data/file/766109/decarbonising-heating.pdf .

[3] A. Del Amo, A. Martínez-Gracia, A. Bayod-Rújula, M. Cañada, Performance analysis and experimental validation of a solar-assisted heat pump fed by photovoltaic-thermal collectors, Energy 169 (2019) 1214–1223.

[4] W. He, X. Hong, X. Zhao, X. Zhang, J. Shen, J. Ji, Operational performance of a novel heat pump assisted solar façade loop-heat-pipe water heating system, Appl. Energy 146 (2015) 371–382.

[5] X. Zhang, X. Zhao, J. Shen, J. Xu, X. Yu, Dynamic performance of a novel solar photovoltaic/loop-heat-pipe heat pump system, Appl. Energy 114 (2014) 335–352.

[6] C. Bai, Z. Han, H. Wei, X. Ju, X. Meng, Qi Fu, The system is able to minimize the ventilation heat loss and provide a unique defrosting approach by using the exhaust waste heat without additional energy consumption, Energy Built Environ. 1 (2020) 1–10.

[7] J. Zhou, X. Zhao, Y. Yuan, J. Li, M. Yu, Yi Fan, Operational performance of a novel heat pump coupled with mini-channel PV/T and thermal panel in low solar radiation, Energy Built Environ. 1 (2020) 50–59.

[8] M. Mohanraj, Y. Belyayev, S. Jayaraj, A. Kaltayev, Research and developments on solar assisted compression heat pump systems – a comprehensive review (Part-B: Applications), Renew. Sustain. Energy Rev. 83 (2018) 124–155.

[9] Solar and Heat Pump Systems Position Paper. Solar Heating and Cooling Programme, International Energy Agency. https://www.iea-shc.org/Data/Sites/1/publications/Postion-Paper-Solar-Heat-Pump-Sytems.pdf

[10] Heat Pumps in London - Greater London Authority. https://www.london.gov.uk/sites/default/files/final_20180167-tgl-180329-gla_heat_pump_research-rev_l_low_res.pdf

[11] L.-.L. Shao, L. Yang, C-Lu Zhang, Comparison of heat pump performance using fin-and-tube and microchannel heat exchangers under frost conditions, Appl. Energy 87 (2010) 1187–1197.

[12] Y. Jiang, J. Dong, M. Qu, S. Deng, Y. Yao, A novel defrosting control method based on the degree of refrigerant superheat for air source heat pumps, Int. J. Refrig. 36 (2013) 2278–2288.

[13] Ju-S Byun, J. Lee, C.-.D. Jeon, Frost retardation of an air-source heat pump by the hot gas bypass method, Int. J. Refrig. 31 (2008) 328–334.

[14] lM.W Liddament, M. Ormea, Energy and ventilation, Appl. Therm. Eng. 18 (1998) 1101–1109.

[15] G.V. Fracastoro, M. Serraino, Energy analyses of buildings equipped with exhaust air heat pumps (EAHP), Energy Build. 42 (2010) 1283–1289.

[16] E. Psimopoulos, E. Bee, J. Widén, C. Bales, Techno-economic analysis of control algorithms for an exhaust air heat pump system for detached houses coupled to a photovoltaic system, Appl. Energy 249 (2019) 355–367.

[17] Z. Liu, W. Li, L. Zhang, Z. Wu, Y. Luo, Experimental study and performance analysis of solar-driven exhaust air thermoelectric heat pump recovery system, Energy Build. 186 (2019) 46–55.

[18] K. Wang, N. Li, J. Peng, X. Wang, C. Wang, M. Wang, A highly efficient solution for thermal compensation of ground-coupled heat pump systems and waste heat recovery of kitchen exhaust air, Energy Build. 138 (2017) 499–513.

[19] M. Thalfeldt, J. Kurnitski, E. Latõšov, Exhaust air heat pump connection schemes and balanced heat recovery ventilation effect on district heat energy use and return temperature, Appl. Therm. Eng. 128 (2018) 402–414.

[20] Z. Zhang, C. Zhang, M. Ge, Y. Yu, A frost-free dedicated outdoor air system with exhaust air heat recovery, Appl. Therm. Eng. 128 (2018) 1041–1050.

[21] A. Chen, H. Liu, C. Ran, C. Wang, Economic analysis on application of exhaust air heat recovery in existing public buildings in the severe cold regions, Int. Forum Energy Environ. Sci. Mater. (2015).

[22] L. Wang, G. Ma, A. Ma, F. Zhou, F. Li, Experimental study on the characteristics of triplex loop heat pump for exhaust air heat recovery in winter, Energy Convers. Manag. 176 (2018) 384–392.

[23] Efficient' heating system left families with big bills". BBC News online. 10 Sep 2012. https://www.bbc.co.uk/news/business-19511637.

[24] D. Liu, F.Y. Zhao, G.F. Tang, Frosting of heat pump with heat recovery facility, Renew. Energy 32 (2007) 1228–1242.

[25] M. Song, S. Deng, C. Dang, N. Mao, Z. Wang, Review on improvement for air source heat pump units during frosting and defrosting, Appl. Energy 211 (2018) 1150–1170.

[26] M. Mohanraj, Ye. Belyayev, S. Jayaraj, A. Kaltayev, Research and developments on solar assisted compression heat pump systems – a comprehensive review (Part A: Modeling and modifications), Renew. Sustain. Energy Rev. 83 (2018) 90–123.

[27] M. Mohanraj, Ye. Belyayev, S. Jayaraj, A. Kaltayev, Research and developments on solar assisted compression heat pump systems – a comprehensive review (Part-B: Applications), Renew. Sustain. Energy Rev. 83 (2018) 124–155.

[28] Heat recovery system efficiencies. https://www.renewableenergyhub.co.uk/main/heat-recovery-systems-information/ heat-recovery-system-efficiencies/#:~:text= Heat%20Recovery%20for%20 Ventilation% 20Systems&text=Thermal%20wheel% 20ventilation%20units%20can,vary%20between%2065%20and%2075%25.&text= Heat%20pipes%20can%20produce%20a,values%20between%2050%20and%2065 %25, 20201025